molecular pharmaceutics

ACS AuthorChoice

Article

pubs.acs.org/molecularpharmaceutics

Terms of Use

An Integrated *in Vitro* Model for Simultaneous Assessment of Drug Uptake, Metabolism, and Efflux

Etienne P. A. Neve,[†] Per Artursson,[‡] Magnus Ingelman-Sundberg,[†] and Maria Karlgren*[,‡]

[†]Section of Pharmacogenetics, Department of Physiology and Pharmacology, Karolinska Institutet, 171 77 Stockholm, Sweden

[‡]Department of Pharmacy, Uppsala University, 751 23 Uppsala, Sweden

Supporting Information

ABSTRACT: The absorption, distribution, metabolism, and excretion (ADME) of drugs *in vivo* are to a large extent dependent on different transport and metabolism routes. Elucidation of this complex transport−metabolism interplay is a major challenge in drug development and at present no *in vitro* models suitable for this purpose are at hand. The aim of this study was to develop flexible, well-controlled, easy-to-use, integrated cell models, where drug transport and drug metabolism processes could be studied simultaneously. HEK293 cells stably transfected with the organic anion transporting polypeptide 1B1 (OATP1B1) were subjected to either transient transfection or adenoviral infection to introduce the genes expressing cytochrome P450 3A4 (CYP3A4), NADPH cytochrome P450 oxidoreductase (POR), cytochrome b_5 (CYB5A), and multidrug resistance protein 1 (MDR1), in different combinations. Thereafter, the time and concentration-dependent transport and metabolism of two well-characterized statins, atorvastatin (acid and lactone forms) and simvastatin (acid form), were determined in the different models. The results show that CYP3A4-dependent metabolism of the more hydrophilic atorvastatin acid was dependent on OATP1B1 uptake and influenced by MDR1 efflux. In contrast, the metabolism of the more lipophilic atorvastatin lactone was not affected by active transport, whereas the metabolism of simvastatin acid was less influenced by active transport than atorvastatin acid. Our results, together with the models being applicative for any combination of drug transporters and CYP metabolizing enzymes of choice, provide proof-of-concept for the potential of the new integrated cell models presented as valuable screening tools in drug discovery and development.

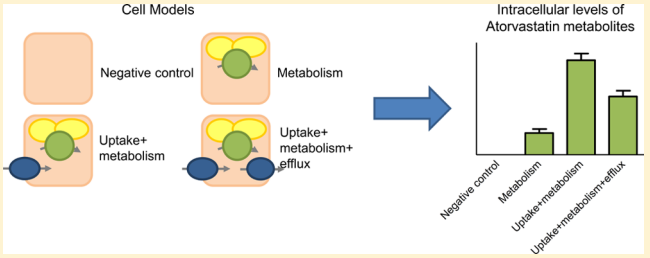

KEYWORDS: *triple transfection, adenovirus infection, drug metabolism, drug transport, OATP1B1, CYP3A4, MDR1, cellular models*

INTRODUCTION

The absorption, distribution, metabolism, and excretion (ADME) of drugs as well as their therapeutic effects are dependent to a large extent on different transport and metabolism routes. In the liver, drug transporters involved in both the active uptake and efflux of drugs and drug metabolites are major determinants of hepatic drug disposition. These transporters determine the access of drug substrates to the large numbers of intracellular drug metabolizing enzymes that metabolize approximately 75% of all prescribed drugs, thereby being the major route of drug elimination.[1] While there is interplay between transport and metabolism processes *in vivo*, these processes are mainly studied separately *in vitro*, for example, with recombinant proteins, cell lines that overexpress transporters, or drug metabolizing enzymes. In more complex and variable *in vitro* models, like primary or cryopreserved hepatocytes, the contribution of the individual transporter or drug metabolizing enzyme is difficult to interpret.[2]

The organic anion transporting polypeptide 1B1 (OATP1B1) and the multidrug resistance protein 1 (MDR1) are two highly expressed transporters of outmost importance to hepatic drug disposition.[3] OATP1B1 is an uptake transporter localized in the sinusoidal plasma membrane responsible for the uptake of anionic drugs.[4,5] Its importance for drug disposition has been emphasized by a number of reports on OATP1B1 mediated drug−drug interactions and the effects of OATP1B1 polymorphisms, in particular for statins.[6,7] The efflux transporter MDR1, localized in the canalicular membrane, is a promiscuous transporter with broad substrate specificity. MDR1 is able to extrude a wide variety of structurally and chemically unrelated compounds of various pharmacological classes.[8−15] Although MDR1 possesses this broad substrate specificity, drug interactions are rather uncommon when MDR1 substrates are coadministered, but inhibition/induction of MDR1 has been reported in animals and humans as a cause of drug−drug interaction.[3,16] MDR1 interactions may be more relevant in the clinic where patients are exposed to multiple MDR1 inhibitors than in controlled drug−drug interaction investigations where only single inhibitors are used.[17]

Cytochrome P450 (CYP) is a large family of drug metabolizing enzymes. From a clinical aspect CYP3A4 is the

Received: April 5, 2013
Revised: June 10, 2013
Accepted: July 3, 2013
Published: July 3, 2013

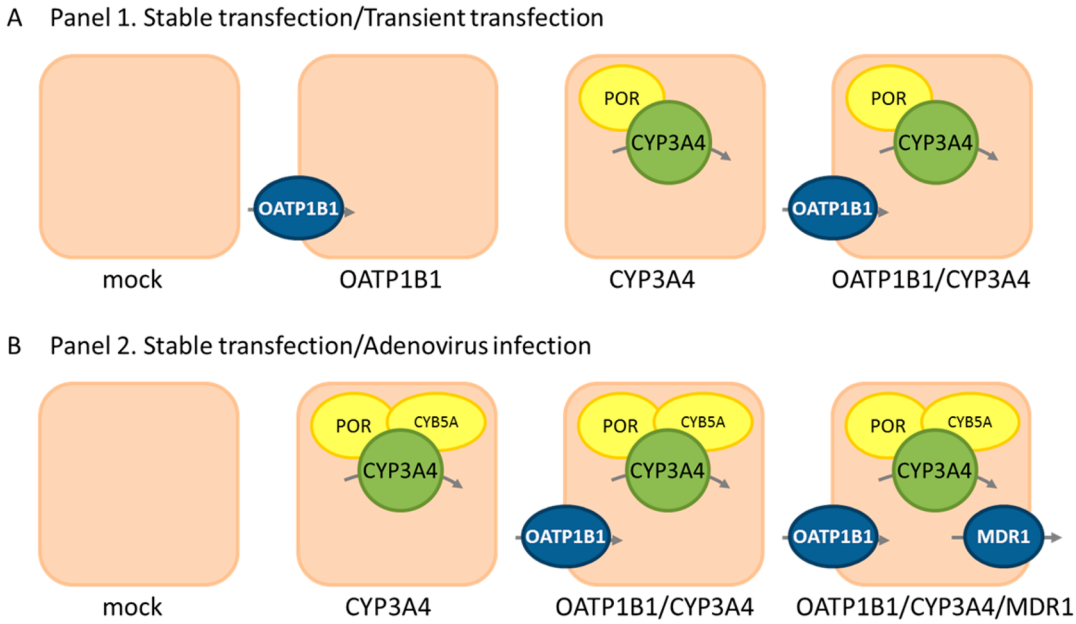

Figure 1. Two panels of integrated cell models developed. (A) Panel 1 is developed using a combination of stable transfection and transient transfection (Lipofectamine 2000). The most advanced cell model in this panel contains the OATP1B1 uptake transporter together with the CYP3A4 metabolizing enzyme and its electron donor NADPH cytochrome P450 oxidoreductase (POR). (B) Panel 2 is developed using a combination of stable transfection and adenoviral infection. Here, the most advanced cell model contains OATP1B1, CYP3A4, and the electron donors POR and cytochrome b_5 (CYB5A) with the addition of the MDR1 efflux transporter.

major member of this family since it is responsible for 60−70% of all phase I metabolism.[18,19] CYP3A4 has similar regulation of and substrate overlap with MDR1, indicating that these two proteins work together to eliminate drugs, which thereby limits the drug bioavailability.[20,21] Such CYP3A4-MDR1 interplay has been seen in knockout mice lacking the genes for Cyp3a and Mdr1. After either oral or intravenous administration of docetaxel, a pronounced effect on the plasma concentration of the drug was seen in these mice, compared to wild-type mice or mice only lacking one of the two proteins.[22,23] Similarly, clinical studies by Benet and colleagues have highlighted how a metabolizing enzyme and a drug transporter also in humans can work together to alter drug bioavailability (for a review see Benet 2009[24]). Recently, when investigating the inhibitory effect of CYP interacting compounds on OATP mediated transport, we discovered that an interaction overlap may also exist between CYP3A4 and the OATPs in humans.[25] In that study 44% of the compounds recommended as CYP3A4 substrates, inhibitors, and/or inducers by the FDA and EMA[26,27] were classified as OATP inhibitors as compared to 31% for all CYP-interacting compounds. This kind of transport-metabolism interplay, together with the fact that the vast majority of all drugs interact with more than one metabolizing enzyme/transporter, clearly shows the pitfalls of studying each process separately *in vitro* and making extrapolations to *in vivo* situations difficult.

The 3-hydroxy-3-methylglutaryl-coenzyme A (HMG-CoA) inhibitors, also known as statins, are widely used as lipid-lowering drugs. Most statins are administered as their active acid form, whereas simvastatin and lovastatin are administered as lactone prodrugs.[28] *In vivo* there is an extensive transformation between the acid and lactone forms of the statins,[29] although in *in vitro* experiments less than ten percent of the compound is transformed.[30] The statins are also a drug class whose ADME properties are affected by OATP1B1, CYP3A4, and MDR1. In particular, polymorphisms in the *SLCO1B1* gene, leading to reduced transporter function, highlight the role of OATP1B1 in statin uptake.[31] OATP1B1 polymorphisms and concomitant use of statins in combination with CYP3A4 inhibitors increase the risk for statin-induced myopathy.[32] Likewise, polymorphism in the *ABCB1* gene encoding MDR1 affects the systemic exposure of atorvastatin and simvastatin acid (cf. Niemi 2010[33]). This results in complex transporter−enzyme interaction patterns which highlight the importance of *in vitro* model systems where interactions between uptake transporters (OATP1B1), drug metabolizing enzymes (CYPs), and efflux transporters (MDR1) are studied under controlled conditions. Several such model systems have been developed, for example, Caco-2 and MDCK cells that overexpress one or two of the three aforementioned components.[34−37] Although valuable, these *in vitro* cell models have several drawbacks including low or no constitutive expression of CYP3A4 and MDR1 and interference from endogenous uptake and efflux transporters.

Here, we have developed two panels of *in vitro* models, which in combination and under controlled conditions, allow the study of both each individual component in detail and the interplay between OATP1B1, CYP3A4, and/or MDR1 (Figure 1). HEK293 cells were chosen as host cell line for creating our models because they do not express significant levels of the most important drug uptake and efflux transporters or CYPs. This minimizes the potential interference from endogenous components.[38] Our most advanced cell model is, to our knowledge, the first cell model combining an uptake transporter, a CYP metabolizing enzyme, and an efflux transporter. This well-defined cell model, containing three of the most important players in hepatic drug disposition, metabolism, and elimination, allows detailed mechanistic studies on different transport and metabolism properties of drugs. In addition, the interplay between transport and metabolism can be evaluated

dx.doi.org/10.1021/mp400202d | *Mol. Pharmaceutics* 2013, 10, 3152−3163

when using this cell model. We evaluated this advanced cell model as well as the rest of the panels of integrated cell models for protein expression and transporter/enzyme activity. In addition, we studied the time and concentration dependency in the transport/metabolism interplay of two statins, atorvastatin (acid and lactone form) and simvastatin (acid form), both with different affinities for the expressed transporters and enzyme.

EXPERIMENTAL SECTION

Cell Cultivation. OATP1B1 HEK293 Flp-In cells and the corresponding mock transfected cells[39] were cultivated in Flp-In-293 medium (Dulbeccos's modified Eagle's medium supplemented with 10% fetal bovine serum (FBS) and 2 mM L-glutamate) supplemented with 75 μg/mL of Hygromycin B (Invitrogen, Rockville, MD). The cells were cultured at 37 °C in an atmosphere of 5% CO_2 and subcultured twice a week. Passage numbers between 10 and 30 were used throughout the study. All cell culture media and reagents were obtained from Invitrogen (Rockville, MD) or Sigma-Aldrich (St. Louis, MO).

First Strand cDNA Synthesis. Total human liver RNA was obtained from Clontech (Mountain View, CA). Reverse transcriptase was performed using the SuperScript III first-strand synthesis supermix according to the manufacturer's instructions (Invitrogen, Rockville, MD).

Cloning and Transient Transfection of CYP3A4 and POR. The CYP3A4 and NADPH cytochrome P450 oxidoreductase (POR) open reading frames (ORFs) were amplified from human liver cDNA with platinum *Pfx* DNA polymerase (Invitrogen, Rockville, MD) and gene-specific primer pairs 5′-CTAGCTCGAGATGGCTCTCATCCCAGACTT-3′/5′-CTAGACGCGTTCAGGCTCCACTTACGGTGC-3′ and 5′-CTAGTCTAGAATGATCAACATGGGAGACTC-3′/5′-CTAGGTCGACCTAGCTCCACACGTCCAGGG-3′. The PCR products were cloned into the *Xho*I/*Mlu*I and *Xba*I/*Sal*I sites of the bicistronic expression vector pIRES (Clontech, Mountain View, CA), respectively. Restriction sites introduced by the primers are underlined. The inserted sequences were verified by DNA sequencing analysis.

HEK293 Flp-In cells stably transfected with OATP1B1, and the corresponding mock cells were grown in T25 flasks and transiently transfected with 10 μg CYP3A4-POR-pIRES expression vector with Lipofectamine 2000 (Invitrogen, Rockville, MD) according to the manufacturer's instructions. OATP1B1 or mock cells transfected with empty pIRES were used as negative controls. Six hours after transfection, the transfection medium was replaced with Flp-In-293 medium without phenol red and Hygromycin B. Eighteen hours later the cells were trypsinized, pelleted by centrifugation, and resuspended in HBSS, pH 7.4 (Sigma-Aldrich, St. Louis, MO) at a concentration of 12×10^6 cells/mL. This cell suspension was used for the subsequent transport and metabolism studies.

Adenovirus. Recombinant adenoviruses were produced using pAd/CMV/V5-DEST Gateway Vectors and a ViraPower Adenoviral Expression System (Invitrogen, Rockville, MD), according to the manufacturer's instructions. Full-length cDNAs of human CYP3A4, cytochrome b_5 type A (CYB5A), and MDR1 were cloned into the pENTR/D-TOPO vector using the pENTR Directional TOPO Cloning kit (Invitrogen, Rockville, MD). POR cDNA was cloned into the pENTR1A Dual Selection Vector. The expression cassettes were transferred from the pENTR Gateway vectors to the adenovirus expression plasmid pAd/CMV/V5-DEST through homologous recombination using Gateway LR Clonase II (Invitrogen, Rockville, MD). All cDNA inserts were verified by sequencing.

Recombinant virus particles were obtained by transfecting *Pac*I linearized pAd/CMV plasmids containing the various cDNAs using Lipofectamine 2000 (Invitrogen, Rockville, MD) into subconfluent 293A producer cells, as described by the manufacturer (Invitrogen, Rockville, MD). After 1−2 weeks, when most of the cells had detached, cells and medium were harvested, and crude viral lysate was prepared by several freeze/thaw cycles. The adenovirus was amplified by infecting 293A producer cells with the crude viral lysate. The amplified virus was purified using the AdEasy Virus Purification kit (Agilent Technologies, Santa Clara, CA), and titer was determined using the AdEasy Viral Titer kit (Agilent Technologies, Santa Clara, CA).

Adenovirus Infection of HEK293 Flp-In Cells. HEK293 Flp-In mock and OATP1B1 cells were plated out in 24-well CellBind plates (Corning, Amsterdam, Netherlands) at a density of 600 000 cells/well in phenol red- and antibiotic-free Flp-In-293 medium. Cells were infected three days after plating with Ad-CYP3A4 (MOI of 4), Ad-POR (MOI of 0.5), and Ad-CYB5A (MOI of 0.5) in the presence or absence of Ad-MDR1 (MOI of 10). Ad-LacZ was used in control infections. Cells were used for uptake/metabolism experiments 24 h postinfection.

Western Blot Analysis. Total cell surface membrane proteins were isolated from OATP1B1- and mock-transfected cells using the Pierce cell surface protein isolation kit (Thermo Fisher Scientific, Waltham, MA), according to the manufacturer's instructions. With this kit, proteins expressed at the cell surface are selectively biotinylated and subsequently purified whereas intracellular proteins are excluded. Protein concentrations were determined using the Pierce 660 nm protein assay supplemented with ionic detergent compatibility reagent (IDCR) (Thermo Fisher Scientific, Waltham, MA). Membrane fractions corresponding to 4 μg of protein were analyzed on SDS-PAGE as described below. Transiently transfected cells or cells infected with Ad-CYP3A4, Ad-POR, Ad-CYB5A, or Ad-MDR1 were solubilized 24 h post-transfection/infection in RIPA buffer and postnuclear supernatant was prepared. Equal amounts of protein were mixed with Laemmli buffer, run on 10% SDS-PAGE, and then transferred to nitrocellulose membranes. The nitrocellulose membranes were incubated with rabbit anti-OATP1B1 antibodies,[40] goat anti-CYP3A4,[41] rabbit anti-POR (AbCam, Cambridge, UK), rabbit anti-CYB5A (Santa Cruz Biotechnology Inc., Santa Cruz, CA), or mouse anti-MDR1 (Sigma-Aldrich, St. Louis, MO), followed by goat anti-rabbit, goat anti-mouse, or rabbit anti-goat conjugated horseradish peroxidase secondary antibodies (Dako Denmark A/S, Glostrup, Denmark). Signals were detected using SuperSignal West Pico Chemiluminescent Substrate (Pierce, Rockford, IL).

Evaluation of Transport and Metabolism. *OATP1B1-Mediated E17βG Transport.* For the determination of estradiol-17β-glucuronide (E17βG) uptake in the OATP1B1 and mock cells transiently transfected with CYP3A4/POR, 100 μL of cell suspension (see above) was added per well in a 96-well MultiScreen filter plate (Millipore, Tullagreen, Ireland). Thereafter the cells were incubated at 37 °C, under gentle agitation for 5 min with 100 μL of a prewarmed E17βG solution in HBSS, giving a final concentration of 1 μCi/mL (24 nM) ^{3}H-E17βG (PerkinElmer, Waltham, MA) and 0.5 μM E17βG (Sigma-Aldrich, St. Louis, MO). As control, cells were

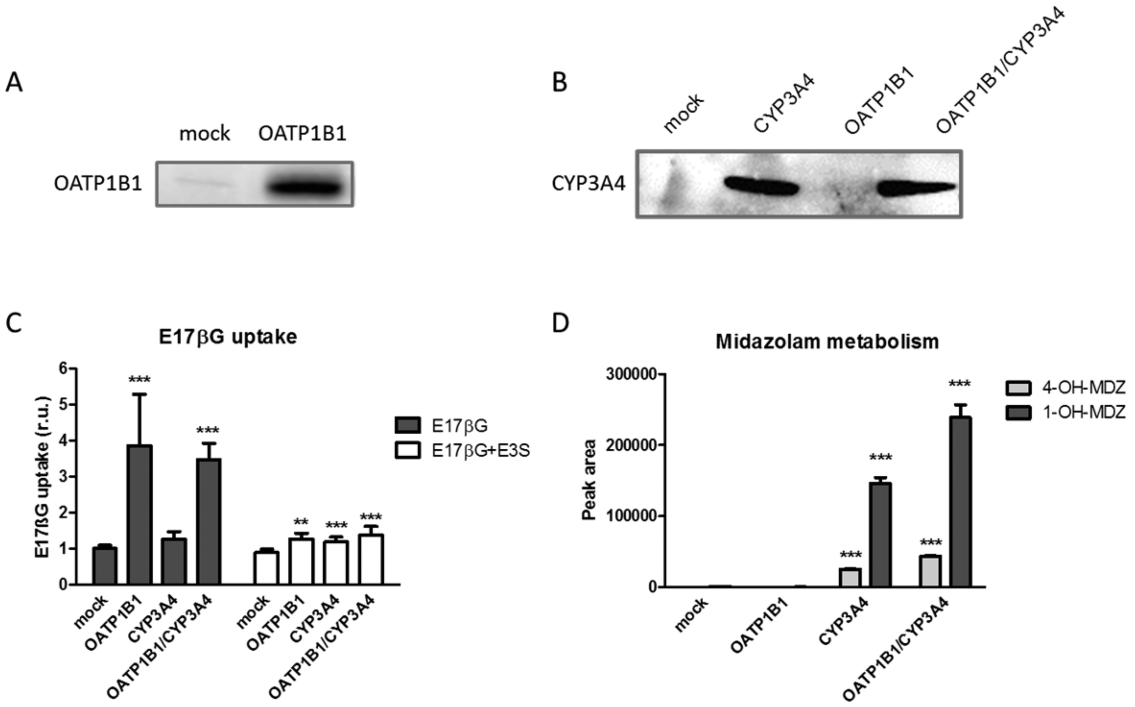

Figure 2. Evaluation of the transporter and the metabolizing enzyme included in the integrated model developed using transient transfection. (A) Western blot analysis of OATP1B1 expression at the cell surface in the stable transfected cells and in the corresponding mock transfected cells. (B) Expression of CYP3A4 after transient transfection of the mock cells and the stable OATP1B1-cells using the CYP3A4-POR-pIRES expression vector or empty pIRES (mock, OATP1B1). (C) Evaluation of OATP1B1 function using estradiol-17β-glucoronide (E17βG) as substrate, with our without addition of 20 μM of the OATP1B1 inhibitor, estrone-3-sulfate (E3S). Cells in suspension were incubated at 37 °C for 5 min. Data are shown as the mean and standard deviation of two independent experiments, each run in quadruplicate. (D) Evaluation of CYP3A4 metabolic activity using 1 μM midazolam. Cells in suspension were incubated at 37 °C for 60 min. Data are shown as mean values and range (n = 2) of one representative experiment. Significant differences as compared to mock cells are shown as *, $p < 0.05$; **, $p < 0.01$; and ***, $p < 0.001$.

incubated with E17βG in the presence of the OATP1B1 inhibitor estrone-3-sulfate (E3S), with a final inhibitor concentration of 20 μM. The transport experiments were terminated by removing the solution by vacuum filtration followed by four washing steps in ice-cold PBS. The cells on the filter plate were subsequently dried, followed by addition of 100 μL of Microscint 40 (PerkinElmer, Waltham, MA), and analyzed using a TopCountNXT scintillation counter (PerkinElmer, Waltham, MA).

For analysis of E17βG uptake the stable OATP1B1 and mock cells were grown and infected with increasing virus concentrations (MOI 0, 2.5, 5, and 10) in 24-well Cellbind plates (Corning, Amsterdam, Netherlands) as described above. At 24 h postinfection, the cells were washed twice with prewarmed HBSS, pH 7.4, followed by 5 min incubation with E17βG/^{3}H-E17βG solution as previously described.[25]

CYP3A4 Mediated Metabolism. For determination of CYP3A4 metabolism in the OATP1B1 and mock cells transiently transfected with CYP3A4/POR, 100 μL of cell suspension was added per well of a 96-well round-bottom plate (Sigma-Aldrich, St.Louis, MO). Thereafter the cells were incubated at 37 °C, under gentle agitation for 60 min with 100 μL of prewarmed 1 or 10 μM midazolam (LGC Standards, Teddington, UK) in HBSS. The metabolism experiments were terminated by transferring the samples to a 96-well MultiScreen filter plate (Millipore, Tullagreen, Ireland) after which the test solution was removed by vacuum filtration. After four washing steps with ice-cold PBS, the samples were extracted by the addition of 200 μL of acetonitrile−H_2O 60:40 spiked with 50 nM warfarin per well. After two minutes the extraction was terminated by vacuum filtration, and the eluates were kept at −20 °C until analysis.

CYP3A4 catalytic activity in cells infected with Ad-CYP3A4, Ad-POR, and Ad-CYB5A was determined 24 h postinfection using the P450-Glo CYP3A4 kit (Promega, Madison, WI) with IPA as a substrate, according to the manufacturer's instructions.

MDR1 Mediated Transport. For the determination of MDR1 mediated transport, cells were infected with Ad-MDR1 MOI 10. At 24 h postinfection, medium containing 0.50 μM calcein-AM (Invitrogen, Rockville, MD) was added, and cells were incubated for 30 min at 37 °C. The incubation was terminated by the removal of medium followed by two washing steps with PBS. Thereafter the cells were lysed in 0.1% Triton X-100/PBS, and calcein fluorescence was determined with a microplate reader (Spectra MAX Gemini, Molecular Devices, Sunnyvale, CA) at 485 nm excitation and 530 nm emission.

Analysis of Statin Transport and Metabolism. For the simultaneous determination of transport and metabolism in the cells transiently transfected with CYP3A4/POR, a 100 μL cell suspension was added per well to a 96-well round-bottom plate (Sigma-Aldrich, St. Louis, MO). After addition of 100 μL of prewarmed atorvastatin acid solution (kindly provided by AstraZeneca, Södertälje, Sweden) in HBSS, giving a final concentration of 3, 10, or 15 μM, the cells were incubated under gentle agitation, at 37 °C for 60 min. The metabolism experiments were terminated by transferring the samples to a 96-well MultiScreen filter plate (Millipore, Tullagreen, Ireland) after which the test solution was removed by vacuum filtration. After four washing steps the samples were extracted as in the

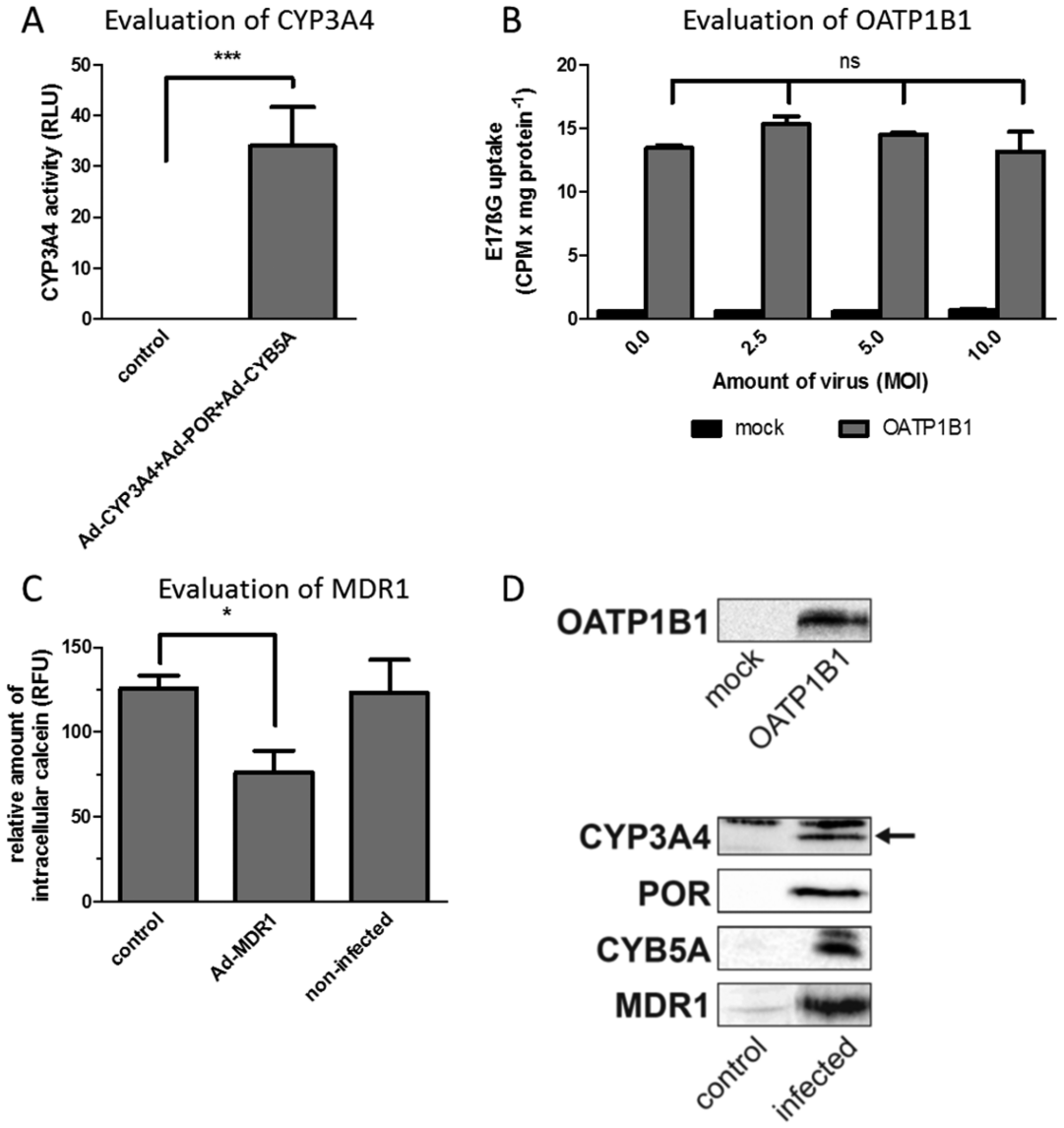

Figure 3. Evaluation of the transporters and the metabolizing enzyme included in the integrated models developed using adenoviral infection. (A) Evaluation of CYP3A4 metabolic activity in cells infected with Ad-CYP3A4, Ad-POR, and Ad-CYB5A using a P450-Glo assay. Cells infected with control virus (Ad-LacZ) served as a negative control. (B) Evaluation of OATP1B1 function using E17βG at different concentrations of virus particles. Infected mock cells are used as negative control. (C) Evaluation of MDR1 function using the MDR1 substrate calcein-AM. Noninfected cells and cells infected with control virus were used as negative controls. (D) Western blot analysis of the expression of OATP1B1, CYP3A4, POR, CYB5A, and MDR1 in the integrated cell model. OATP1B1 expression is determined in total cell lysates of the cells stably transfected with OATP1B1 and the corresponding mock cells (upper panel). Lower panels show the expression of CYP3A4 (specific band marked with an arrow), POR, CYB5A, and MDR1 in total cell lysates obtained from the OATP1B1 cells infected with Ad-CYP3A4, Ad-POR, Ad-CYB5A, and Ad-MDR1, respectively. OATP1B1 cells infected with Ad-LacZ served as a control. Data are shown as mean and standard deviation (n = 3). ns, not significant; *, $p < 0.05$; **, $p < 0.01$; and ***, $p < 0.001$.

midazolam experiment. The test solutions and eluates were kept at −20 °C until analysis.

For simultaneous determination of transport and metabolism, cells infected with Ad-CYP3A4, Ad-POR, Ad-CYB5A, and Ad-MDR1 grown in 24-well plates were washed twice with prewarmed HBSS, pH 7.4, and incubated at 37 °C with a solution containing atorvastatin acid, atorvastatin lactone or simvastatin acid in HBSS, giving final concentrations of 3, 15, or 30 μM, for 10 or 60 min. The incubation was terminated by the removal of the test solution followed by three washing steps with ice-cold PBS. After the washing, 150 μL of acetonitrile was added per well and allowed to evaporate at room temperature. The cells and the test solutions were then stored at −20 °C for later analysis.

For the adenoviral experiments total protein content per well was measured using the BCA Protein Assay Reagent Kit (Pierce Biotechnology, Rockford, IL, USA) according the manufacturer's instructions. Based on the number of cells used in the transport/metabolism experiments (transiently transfected cells) or on the obtained protein data (cells infected with adenovirus), all intracellular amounts of substrates and metabolites were adjusted to reflect the concentrations in the total cell volume (6.5 μL/mg protein[42]).

LC-MS/MS Analysis. The dried cells were extracted for 10 min using acetonitrile:H_2O 60:40 spiked with 50 nM warfarin

and intracellular concentrations of the test compound and metabolites were analyzed using UPLC-MS/MS as previously described.[39] For analysis of extracellular concentrations of test compounds and metabolites the saved test solutions (see above) were diluted 2 and 50 times with acetonitrile:H_2O 60:40 spiked with 50 nM warfarin and thereafter subjected to UPLC-MS/MS analysis.

Statistics. All experiments were performed in at least duplicates in at least two independent experiments. In all experiments, ANOVA and Dunnett's multiple comparison tests were used to ensure significant differences between the different conditions.

RESULTS

Establishment of Integrated Cell Models Using Transient Transfection. Western blot analyses of isolated cell surface proteins from the stably transfected OATP1B1 HEK293 Flp-In cells and mock cells showed that the OATP1B1 transfected cells specifically expressed the OATP1B1 protein which was localized at the plasma membrane (Figure 2A). Western blot analyses of total cell extracts from the cells transiently transfected with CYP3A4 and POR showed specific expression of the CYP3A4 protein in the CYP3A4 transfected cells, with equal expression in both CYP3A4 and OATP1B1/CYP3A4 cells (Figure 2B).

OATP1B1 function in the transiently transfected cells was validated using the OATP1B1 substrate E17βG. There was a significantly higher uptake of E17βG in the OATP1B1-expressing cells compared to mock cells. In addition, no alteration in OATP1B1-mediated uptake, as a result of the transient CYP3A4 transfection, could be seen (Figure 2C). The activity of the introduced CYP3A4 enzyme was evaluated using the CYP3A4 substrate midazolam. In the transiently transfected cells, the 1-hydroxy- and 4-hydroxy-midazolam metabolites were specifically identified in those cells transfected with the CYP3A4/POR construct (Figure 2D). Metabolite levels were higher in the cells also expressing the OATP1B1 transporter, for both midazolam concentrations (1 and 10 μM) (Figure 2D and data not shown).

Establishment of Integrated Cell Models Using Adenovirus. The adenoviral constructs, Ad-CYP3A4, Ad-POR, Ad-CYB5A, and Ad-MDR1, were initially titrated to optimize the functional expression of CYP3A4 and MDR1. Different amounts of Ad-CYP3A4 and the electron donors Ad-POR and Ad-CYB5A were used to infect mock and OATP1B1 cells. Thereafter the CYP3A4 catalytic activity was determined 24 h postinfection using the P450-Glo CYP3A4 kit. Optimal CYP3A4 activity occurred when using a combination of Ad-CYP3A4 MOI 4 and Ad-POR MOI 0.5 (Supplementary Figure 1A), in both mock and OATP1B1 cells. The addition of Ad-CYB5A MOI 0.5 further enhanced the CYP3A4 catalytic activity (Supplementary Figure 1B). Therefore, a combination of Ad-CYP3A4 MOI 4, Ad-POR MOI 0.5, and Ad-CYB5B MOI 0.5 was chosen for all subsequent experiments. In fact, no CYP3A4 dependent activity could be detected in cells infected with control virus (Ad-LacZ), but high CYP3A4 activity was detected in the cells infected with Ad-CYP3A4, Ad-POR, and Ad-CYB5A (Figure 3A).

The activity of the stably expressed OATP1B1 in the infected cells was evaluated using the OATP1B1 substrate E17βG. There was a significantly higher uptake of E17βG in the OATP1B1-expressing cells compared to the mock cells. In addition, increasing concentrations of control viral particles (Ad-LacZ) did not alter the OATP1B1 mediated uptake nor did they increase the permeability of the mock cells (Figure 3B).

The functional expression of Ad-MDR1 was monitored by measuring the intracellular accumulation of calcein. Ad-MDR1- and Ad-LacZ- (control) infected cells were incubated 24 h postinfection with the cell-permeable MDR1 substrate, calcein-AM (Figure 3C). Infection with Ad-MDR1 MOI 10 significantly reduced the amount of calcein, which indicates that active MDR1 was being expressed.

Finally, the protein expression of OATP1B1, CYP3A4, POR, CYB5A, and MDR1 was confirmed by Western blot and immunofluorescence analyses of mock and OATP1B1 cells infected with each of the different adenoviruses. All four adenoviral-transduced constructs were expressed in the infected cells (Figure 3D) but not in the controls. In addition, the expression and cellular localization of OATP1B1 (expressed in the plasma membrane), the virally transduced proteins (CYP3A4, POR, CYB5A, all localized in the endoplasmic reticulum), and MDR1 (expressed in the plasma membrane) were confirmed by immunofluorescence (Supplemental Figure 2). In contrast to human hepatocytes, where OATP1B1 is localized to the basolateral membrane and MDR1 is localized to the apical membrane, immunofluorescence analyses showed that in the nonpolarized HEK293 cells both transporters display cell surface localization without localization to a specific part of the plasma membrane (Supplemental Figure 2). In addition, for MDR1 also some intracellular staining was seen.

Atorvastatin Acid Transport and Metabolism. Atorvastatin acid was chosen as the primary compound for evaluation of the new integrated cell models (Figure 1). On the basis of literature[43] and previous in-house experiments, we anticipated that atorvastatin acid (for which active uptake, especially via OATP1B1, has been suggested as the rate-limiting step), would show higher metabolite levels in the cell models expressing both OATP1B1 and CYP3A4 compared to cell models without the OATP1B1 transporter.

Incubation of the mock and OATP1B1-expressing cells transiently transfected with CYP3A4 and POR with increasing concentrations of atorvastatin acid for 60 min resulted in significantly higher formation of atorvastatin acid metabolites in the integrated cell model containing OATP1B1, CYP3A4, and POR (OATP1B1/CYP3A4 model) (Figure 4, Supplemental Table 1). In this cell model, up to 31-fold higher levels of intracellular hydroxyl-atorvastatin acid were detected compared to the CYP3A4 and POR containing cell model without the OATP1B1 transporter (CYP3A4 model). The greatest differences (31-fold) between these two cell models were for incubations with the lowest atorvastatin acid concentration, that is, 3 μM (Figure 4A). At concentrations of 10 and 15 μM atorvastatin acid (Figure 4B,C), the differences in intracellular hydroxyl-atorvastatin acid concentrations in the cell models were reduced, suggesting saturation of the uptake transporter at these higher substrate concentrations. Higher levels of hydroxyl-atorvastatin acid were also detected in the extracellular compartment of the OATP1B1/CYP3A4 model compared to the CYP3A4 model. However, the extracellular metabolite levels were much lower than the intracellular levels for all atorvastatin concentrations and cell models tested. Considering the long incubation time and the high concentration gradient between the intracellular and extracellular compartments, the observed increase in extracellular metabolite levels is most likely the result of passive permeability.

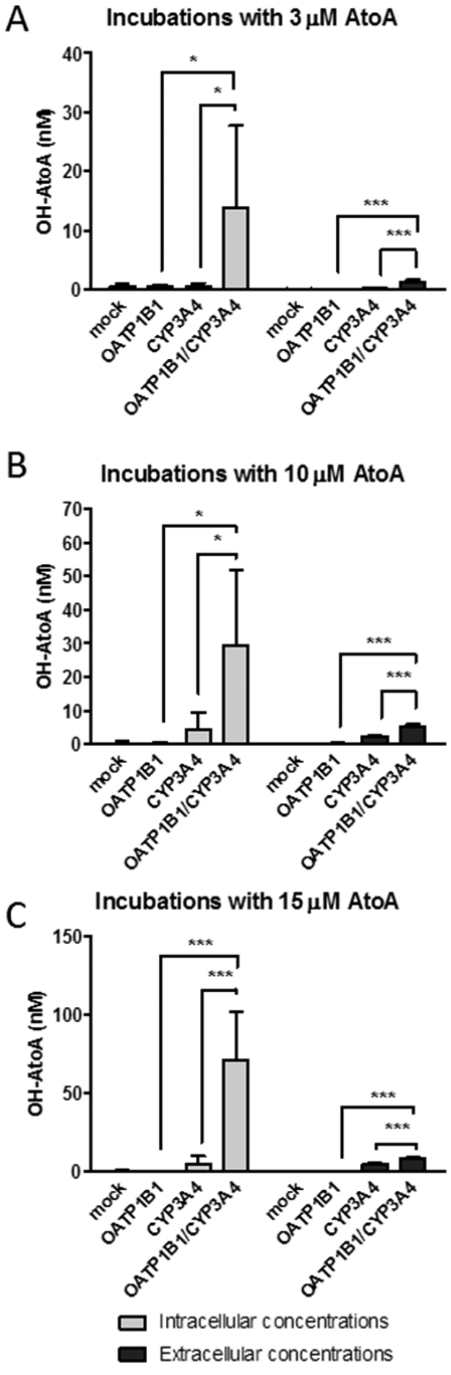

Figure 4. Transport−metabolism interplay in the integrated cell models developed by transient transfection. Intracellular and extracellular concentrations in nM of hydroxyl-atorvastatin acid (OH-AtoA) after incubation with (A) 3, (B) 10, and (C) 15 μM atorvastatin acid for 60 min. Data are shown as the mean and standard deviation ($n = 4$) of one representative experiment. *, $p < 0.05$; **, $p < 0.01$; and ***, $p < 0.001$.

For the cell models developed using adenoviral infections, initial experiments with atorvastatin acid were performed using all possible transporter-metabolizing enzyme combinations (i.e., mock, CYP3A4, MDR1, CYP3A4/MDR1, OATP1B1, OATP1B1/CYP3A4, OATP1B1/MDR1, and OATP1B1/CYP3A4/MDR1, see Supplemental Figure 3). As no or only low metabolite levels were detected in several of the models the mock, CYP3A4, OATP1B1/CYP3A4, and OATP1B1/CYP3A4/MDR1 models were selected for use in all subsequent experiments. Using the selected models, incubations with increasing concentrations of atorvastatin acid at 10 and 60 min showed significantly higher levels of intracellular metabolites in the OATP1B1/CYP3A4 model compared to the CYP3A4 model (Figure 5A and Supplemental Table 2). In the 60 min incubations with 3 μM and 15 μM atorvastatin acid, the increase in intracellular metabolite concentration was most pronounced, with 122 nM and 2220 nM hydroxyl-atorvastatin acid in the CYP3A4 model compared to 533 nM and 3500 nM in the OATP1B1/CYP3A4 model, respectively (Supplemental Table 2). For the OATP1B1/CYP3A4/MDR1 model (which also expressed the MDR1 efflux transporter) intracellular metabolite concentrations were reduced to 328 nM, for 3 μM incubations (Figure 5A and Supplemental Table 2) and to 1950 nM for 15 μM incubations (Supplemental Table 2) compared to the OATP1B1/CYP3A4 model. A similar pattern for the atorvastatin metabolite levels was observed in the extracellular compartment for OATP1B1/CYP3A4 and OATP1B1/CYP3A4/MDR1 models. In addition, the intracellular levels of the mother compound, atorvastatin acid, were dependent on the presence of OATP1B1, especially at low concentrations and at short incubation times (Figure 5B and Supplemental Table 2). However, no significant difference in levels of the mother compound could be seen after addition of the MDR1 transporter. At the higher atorvastatin concentrations (15 and 30 μM) and 60 min incubation, no difference could be seen in intracellular atorvastatin acid levels for any of the cell models. The metabolite levels in the CYP3A4 model and the OATP1B1/CYP3A4 model did not rise with increasing concentration of atorvastatin, most likely because the OATP1B1 transporter-mediated uptake of atorvastatin acid was saturated (Supplemental Table 2). It should be noted, however, that the clinically relevant concentration of atorvastatin acid ($C_{max,unbound}$ = 2 nM[44,45]) is far below these saturating levels. In general our results concur with the literature that reports atorvastatin acid as a substrate for OATP1B1, CYP3A4, and MDR1[32] and where OATP1B1-mediated uptake is suggested to be the rate-limiting factor of atorvastatin hepatic elimination.[43]

The stable OATP1B1 cells have previously been evaluated with different substrates with good reproducibility between experiments.[25,39] Comparisons across experiments show that the adenovirus based models also have good reproducibility for the metabolism/transport of atorvastatin. CYP3A4 activity, as indicated by the intracellular atorvastatin acid metabolite concentration in the CYP3A4 models, has a variability of ±10% as compared to the average intracellular concentration across experiments (Supplementary Figure 4A.). Also for the OATP1B1/CYP3A4/MDR1 model, the intracellular concentrations of atorvastatin acid metabolites show low interexperimental variability, although higher as compared to the CYP3A4 model (Supplementary Figure 4B). These data indicate that the protein expression levels in the models used in the present study display little variation and confirm the reproducibility of our cell models.

Atorvastatin Lactone Transport and Metabolism. In contrast to atorvastatin acid, previous studies suggest that the pharmacologically inactive and more lipophilic atorvastatin lactone is less dependent on both the OATP1B1 and MDR1 transporter, whereas it is a very good substrate for the CYP3A4 enzyme.[29,46−48] Incubation of the adenovirus-infected cell models for 10 or 60 min with increasing concentrations of

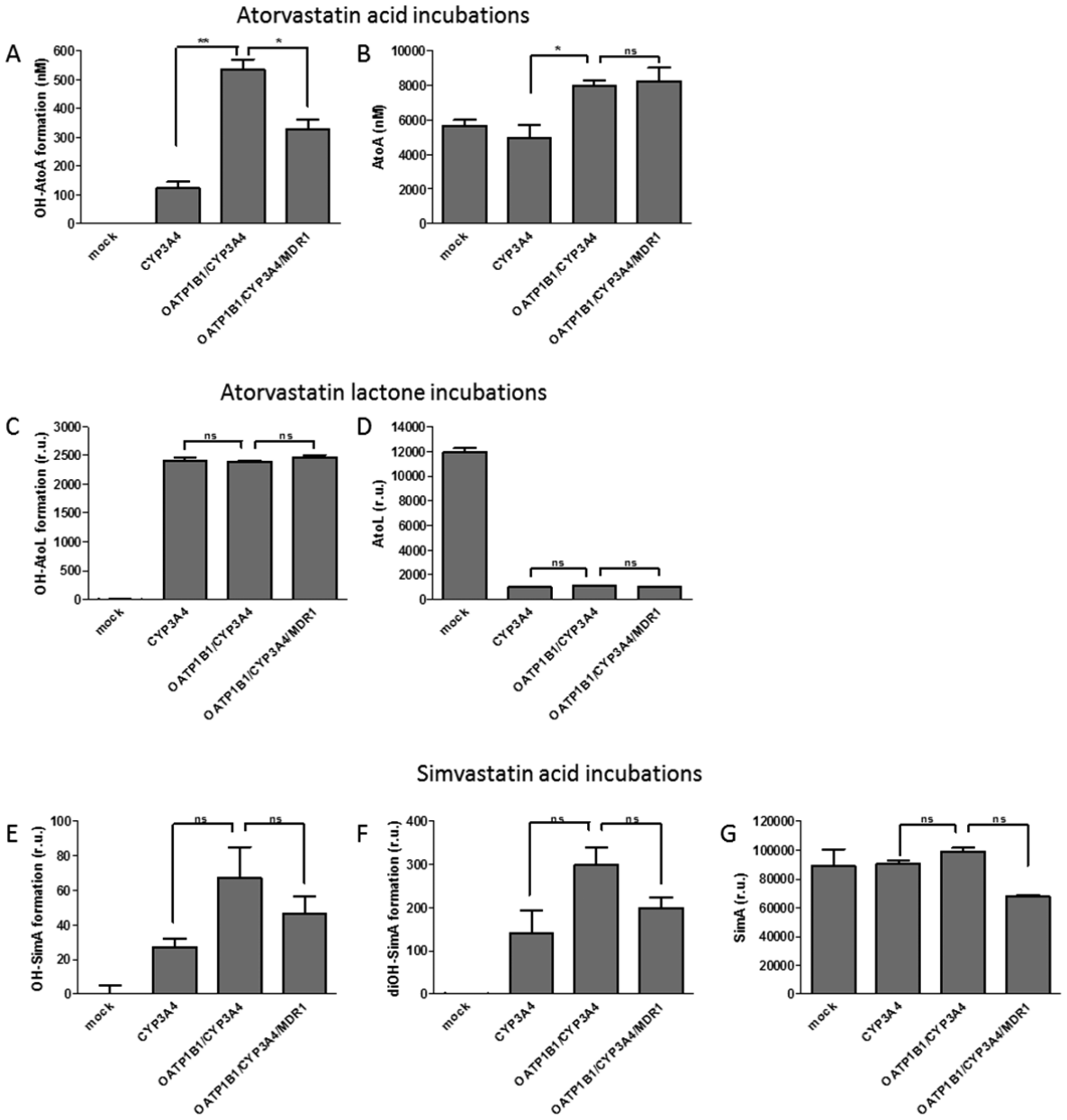

Figure 5. Transport−metabolism interplay in the integrated cell models developed by adenovirus infection. Intracellular concentrations in nM of (A) hydroxyl-atorvastatin acid (OH-AtoA) and (B) atorvastatin acid (AtoA) after incubation with 3 μM atorvastatin acid for 60 min. Intracellular concentrations in relative units of (C) hydroxyl-atorvastatin lactone (OH-AtoL) and (D) atorvastatin lactone (AtoL) after incubation with 3 μM atorvastatin lactone for 60 min. Intracellular concentrations in relative units of (E) hydroxyl-simvastatin acid (OH-SimA), (F) dihydroxyl-simvastatin acid (diOH-SimA), and (G) simvastatin acid (SimA) after incubation with 3 μM simvastatin acid for 60 min. Data are shown as mean and range (n = 2) of one representative experiment. ns, not significant; *, $p < 0.05$; **, $p < 0.01$; and ***, $p < 0.001$.

atorvastatin lactone showed no significant differences in intracellular metabolite levels for the different CYP3A4-containing cell models. This lack of difference was independent of atorvastatin lactone concentration, incubation time, or presence of uptake or efflux transporters (Figure 5C, Supplemental Table 3). The amount of intracellular hydroxyl-atorvastatin lactone ranged from 23.6 to 24.5 (relative units) (10 min incubation with 3 μM atorvastatin lactone) up to 543−611 (60 min incubation with 30 μM atorvastatin lactone). The intracellular atorvastatin lactone concentration was clearly lower in the cell models with CYP3A4-mediated metabolism compared to those without CYP3A4 activity (Figure 5D). This illustrates that atorvastatin lactone is a good CYP3A4 substrate. In summary, our cell model results are in agreement with previous findings regarding transport and metabolism for this compound.[32,46−48]

Simvastatin Transport and Metabolism. Simvastatin acid, just like atorvastatin acid and lactone, is metabolized by CYP3A4;[32] however, it is less dependent on active transport than atorvastatin acid.[30,46] When the adenovirus-infected panel of cell models were incubated with increasing concentrations of simvastatin acid for 10 and 60 min, the intracellular levels of the two simvastatin acid metabolites, hydroxyl-simvastatin acid and dihydroxyl-simvastatin acid, showed a similar, but non-significant, trend compared to atorvastatin acid, that is, higher metabolite levels in the presence of the OATP1B1 transporter

dx.doi.org/10.1021/mp400202d | Mol. Pharmaceutics 2013, 10, 3152−3163

and a subsequent decrease with the addition of the MDR1 transporter (Figure 5E,F vs A, Supplementary Table 4). The intracellular simvastatin acid concentrations were unaffected by the presence of CYP3A4, OATP1B1 or MDR1 (Figure 5G, Supplementary Table 4). This lack of significant differences for the CYP3A4-containing cell models is not surprising in light of other studies comparing the transport and metabolism of atorvastatin acid with simvastatin acid. In those studies the more lipophilic simvastatin acid is not as dependent on OATP1B1-mediated uptake as the more hydrophilic (and hence membrane impermeable) atorvastatin acid.[28,32] Moreover, atorvastatin acid is a better MDR1 substrate compared to simvastatin acid.[30,46]

DISCUSSION

In this paper, we used a combination of stable and transient transfection/adenovirus infections to develop a series of flexible integrated cell models to study the interplay between drug transport and metabolism under well controlled conditions. To our knowledge, these are the first cellular models where the interdependence between drug uptake and efflux transporters of choice and the most important drug metabolizing enzyme, CYP3A4, can be studied without bias from endogenous processes. These models can be used for both mechanistic studies and for determination of the specific transporters/enzymes involved in drug disposition and elimination of drugs and their metabolites.

Cell models containing different combinations of drug uptake and efflux transporters have been developed earlier for the study of vectorial transport of drugs.[36,49] Recently a model combining CYP3A4 and MDR1 in MDCK cells was suggested to be better suited to predict drug−drug interactions since it incorporates both drug metabolism and efflux.[37] In addition, another cell model with MDCK cells, which combines drug transporters and the phase II enzyme UGT1A1, has been used to demonstrate the interplay between phase II metabolism and drug transporters.[35] During the review of this paper Fahrmayr et al.[50] developed and evaluated a stable MDCK cell model expressing a combination of OATP1B1, CYP3A4, UGT1A1 and the multidrug resistance protein 2 (MRP2). With cell monolayers grown on filters this type of cell model represents a valuable tool for studying the vectorial interplay between transport and metabolism processes. However, being based solely on stable transfection, this model does not have the same flexibility as the transient or adenovirus based models described here. In addition the Fahrmayr model, as well as the majority of the existing cell models mentioned above, are based on the canine cell line MDCK, in which the obtained results may potentially be hampered by the presence of endogenous transporters and drug metabolizing enzymes. Many efforts have been made to reduce the contribution of these endogenous components, such as the endogenous expression of canine MDR1 in MDCK cells in order to reduce its contribution to the overall efflux.[51] Other approaches used to determine the contribution of specific transporters in drug disposition include the use of different RNA interference techniques in human hepatocytes.[52−54] Although a valuable *in vitro* tool to determine how the individual contribution of one uptake or efflux transporter affects drug transport such methods also have several drawbacks. This is mainly due to the innate complexity of the human hepatocytes, the incomplete silencing of the gene of interest (most studies describe approximately 10% mRNA remaining and, depending on half-life, even higher remaining levels of the corresponding protein (cf. Liao et al. 2010 and Yue et al. 2009[52,54])), and the unpredictable off-target effects.[48,52] Our models use the HEK293 cell line, which is of human origin and has very low endogenous background from drug-metabolizing enzymes and drug transporters.[38] As a result there is no need in our cellular system to inhibit or correct for endogenous transporter activities as with MDCK cells.

In the present paper we have used two different approaches to develop panels of integrated cell models that are able to predict transport and metabolism of drugs and new drug candidates. We decided for HEK293 cells as the host cell line since they have low or no endogenous expression of drug transporters and drug metabolizing enzymes. However, they also contain low endogenous levels of the CYP electron donors POR and CYB5A (Figure 3D) which are essential for CYP3A4 functionality. Initially, we utilized stable and transient transfections to generate cell models; both methods are commonly used in the studies of a single transporter or a metabolizing enzyme. The ORF for the CYP electron donor POR was added to the CYP3A4 expression plasmid used for the transient transfection. Indeed, lower levels of CYP3A4 activity were detected in the absence of POR cotransfection (data not shown), demonstrating that HEK293 cells have low endogenous POR levels. Our second approach involved a combination of stable transfection and adenoviral infection. With this approach, more components (in this case CYB5A and MDR1 (see Figure 1B)) could be added to the cell model without affecting toxicity, cell attachment, or OATP1B1 function, all of which can occur during transient transfection. The CYP3A4 catalytic activity was optimized by coexpression of its two essential redox partners, POR and CYB5A. As a result, our models are not limited by low endogenous POR and CYB5A levels, which can be a major drawback for many CYP *in vitro* models.

The different integrated cell models developed here were evaluated using atorvastatin acid, atorvastatin lactone, and simvastatin acid, three well-studied and characterized compounds each with different affinities for the transporters and the drug metabolizing enzyme. Atorvastatin acid is a good substrate for OATP1B1,[43] MDR1,[32] and CYP3A4,[47] while the more hydrophobic atorvastatin lactone is only a good CYP3A4 substrate[47] and is not dependent on the OATP1B1 or MDR1 transporters.[46,48] Simvastatin acid, on the other hand, is a substrate for OATP1B1, MDR1, and CYP3A4, although simvastatin acid has lower affinity than atorvastatin acid for these two transporters.[28,30,32,46]

Indeed, when these cell models were incubated with atorvastatin acid, higher metabolite levels in the OATP1B1 and CYP3A4 containing models (OATP1B1/CYP3A4), compared to those without OATP1B1 were observed, both at the intracellular and extracellular levels. Conversely, in the adenovirus-infected OATP1B1/CYP3A4/MDR1 model with the efflux transporter MDR1, the intracellular atorvastatin acid metabolite levels were reduced. However, the extracellular atorvastatin acid metabolite levels also decreased in the OATP1B1/CYP3A4/MDR1 model compared to the one without the efflux transporter. Although significant differences in metabolite levels were seen for these two cell models, no significant difference in intracellular levels was seen for the mother compound. Hence, no clear conclusions can be drawn regarding the mechanism responsible for the lower metabolite levels. The significant decrease in both intracellular and extracellular metabolite levels in the OATP1B1/CYP3A4/

MDR1 model indicates that the intracellular reduction of metabolites was not due to metabolite efflux.

After incubations with atorvastatin lactone, the intracellular substrate concentrations were higher than the extracellular ones, confirming previous observations that the lactone has high permeability.[29] Furthermore, the intracellular lactone levels were independent of the expression of the OATP1B1-uptake transporter. In contrast, there was a major difference in the atorvastatin lactone levels in cell models expressing CYP3A4 compared to the cell models lacking this enzyme. This reflects the extensive metabolic capacity of the CYP3A4 containing models. The metabolite, hydroxyl-atorvastatin lactone, showed a corresponding pattern in these cell models: no effect of OATP1B1, high intracellular levels in all cell models expressing CYP3A4, and no dependence of MDR1. As mentioned, atorvastatin lactone is a non-OATP1B1 substrate[48] and has a lower MDR1 efflux ratio *in vitro* than atorvastatin acid.[46] Also, it has a higher passive permeability as compared to the acid form a consequence of its higher lipophilicity.[29] Its higher reliance on passive membrane permeability, together with its significantly higher affinity for CYP3A4 mediated metabolism,[47] can explain the lack of difference in the intracellular metabolite levels for the different cell models.

Simvastatin acid, the third compound used for the evaluation of the adenovirus-infected cell models, is reported to be both a nonsubstrate and substrate of OATP1B1 *in vitro*.[55,56] This discrepancy is most likely a result of the relatively high lipophilicity of simvastatin acid. When simvastatin is administered as a lactone prodrug in humans, individuals heterozygous or homozygous for OATP1B1 reduced-function alleles show higher simvastatin acid plasma concentrations and increased simvastatin-related adverse effects, implicating a role for OATP1B1 in the uptake of simvastatin acid *in vivo*.[31,57] In our study, no significant differences in simvastatin acid levels could be seen for any of the cell models. Also for the two simvastatin metabolites, hydroxyl-simvastatin acid and dihydroxyl-simvastatin acid, no significant differences could be seen in the cell models with or without OATP1B1, although the levels were generally lower in the cell models without OATP1B1. Similarly, no significant differences in metabolite levels could be detected in the cell models with or without MDR1, although overall the levels were lower in those containing MDR1. It is possible that the potential effect of active transport on both simvastatin acid and simvastatin metabolite levels was masked by the high degree of passive permeability. Altogether our observations are in agreement with previous studies where simvastatin acid has a lower affinity for the two investigated transporters and a higher passive permeability than atorvastatin acid.[30,32,46]

Finally, a comparison of the atorvastatin acid results from the two different cell model approaches shows that the adenovirus-infected cell model has higher metabolite levels, most likely due to higher transfection efficiency and the addition of CYB5A. In addition, the ratio of extracellular/intracellular metabolites is lower, which might indicate higher integrity of the plasma membrane using the stable transfection/adenoviral infection approach. In summary, evaluation of these panels of cell models shows that our methods (i.e., a combination of stable transfection and adenovirus infection) for expression of the transporters and metabolizing enzyme in combination with the unlimited access of the CYP redox partners, gives well-functioning, easily interpretable, flexible cell models applicable for any combination of drug transporters and CYP enzymes of choice.

In conclusion, the cellular models developed in the present study make it possible to study the uptake, metabolism, and efflux of candidate drugs and their metabolites. Drug metabolites tend to be more hydrophilic that the parent compound, hence a model where the metabolite efflux can be studied easily and specifically would be very valuable. Today, even when using, for example, human hepatocytes, which are regarded as the "gold standard" for transport and metabolism studies, the mechanistic elucidation of transport−metabolism interplay of drugs and drug metabolites is often unresolvable. This is a consequence of too complex models, models that have not been completely characterized, or the lack of specific inhibitors for the transporters and drug metabolizing enzymes. The type of flexible cell models developed here can be combined with quantitative protein analysis for accurate scaling of the *in vivo* situation using a similar approach like the one previously used for predicting the contribution of different OATP transporters to the intrinsic uptake clearance of atorvastatin and the subsequent effect of potential drug−drug interactions.[25] Utilizing such an approach, taking both *in vitro* and *in vivo* protein expression levels as well as *in vitro* kinetics into consideration, will hopefully lead to better predictions of mechanistic interplay between transport and metabolism not only *in vitro* but also *in vivo*. We anticipate that by using this approach medium-throughput cellular systems can be developed, which, in drug discovery, could be a valuable tool in determining the interactions between transport and metabolism for both drugs and drug metabolites.

■ ASSOCIATED CONTENT

Supporting Information

Materials and methods describing the optimization of the adenoviral infection and the immunofluorescence analysis, tables containing intracellular and extracellular concentrations from the statin experiments shown in Figures 4 and 5, as well as figures showing results for the optimization of adenoviral infection, immunofluorescence analysis, transport−metabolism interplay between all possible integrated cell models (developed using adenoviral infection), and reproducibility between experiments. This material is available free of charge via the Internet at http://pubs.acs.org.

■ AUTHOR INFORMATION

Corresponding Author

*Department of Pharmacy, Uppsala University, Box 580 SE-751 23, Uppsala, Sweden. E-mail: maria.karlgren@farmaci.uu.se. Phone: +46-18 471 41 49. Fax: +46-18 471 42 23.

Author Contributions

Both research groups contributed equally to this work.

Notes

The authors declare no competing financial interest.

■ ACKNOWLEDGMENTS

This work was supported by AstraZeneca, the Swedish Governmental Agency for Innovation Systems, the Swedish Research Council, the Swedish Fund for Research Without Animal Experiments, the Lars Hierta Memorial Foundation and the O. E. and Edla Johansson Scientific Foundation. The authors are indebted to Richard Svensson, Maria Mastej, Elin Svedberg and Margareta Porsmyr-Palmertz for their valuable

contribution in UPLC-MS/MS analysis, cell cultivation, viral infection, etc. OATP1B1 and CYP3A4 antibodies were kindly provided by Drs. Jörg König and Maria Almira Correia, respectively.

■ ABBREVIATIONS

ABCB1, ATP-binding cassette subfamily B member 1; ADME, Absorption, distribution, metabolism, and excretion; CYB5A, Cytochrome b_5 type A; CYP3A4, Cytochrome P450 3A4; E17βG, Estradiol-17β-glucuronide; E3S, Estrone-3-sulfate; HBSS, Hank's balanced salt solution; HEK293, Human embryonic kidney 293; HMG-CoA, 3-hydroxy-3-methylglutaryl-coenzyme A; MDCK, Madin-Darby canine kidney; MDR1, Multidrug resistance protein 1; MOI, Multiplicity of infection; OATP1B1, Organic anion transporting polypeptide 1B1; PBS, Phosphate-buffered saline; POR, NADPH cytochrome P450 oxidoreductase; SDS-PAGE, Sodium dodecyl sulfate polyacrylamide gel electrophoresis; *SLCO1B1*, Solute carrier organic anion transporter family member 1B1; UPLC-MS/MS, Ultra-performance liquid chromatography tandem mass spectrometry

■ REFERENCES

(1) Wienkers, L. C.; Heath, T. G. Predicting in vivo drug interactions from in vitro drug discovery data. *Nat. Rev. Drug Discovery* **2005**, *4*, 825−33.

(2) Keogh, J. P. Membrane transporters in drug development. *Adv. Pharmacol.* **2012**, *63*, 1−42.

(3) Giacomini, K. M.; Huang, S. M.; Tweedie, D. J.; Benet, L. Z.; Brouwer, K. L.; Chu, X.; Dahlin, A.; Evers, R.; Fischer, V.; Hillgren, K. M.; Hoffmaster, K. A.; Ishikawa, T.; Keppler, D.; Kim, R. B.; Lee, C. A.; Niemi, M.; Polli, J. W.; Sugiyama, Y.; Swaan, P. W.; Ware, J. A.; Wright, S. H.; Yee, S. W.; Zamek-Gliszczynski, M. J.; Zhang, L. Membrane transporters in drug development. *Nat. Rev. Drug Discovery* **2010**, *9*, 215−36.

(4) Hagenbuch, B.; Meier, P. J. Organic anion transporting polypeptides of the OATP/ SLC21 family: phylogenetic classification as OATP/ SLCO superfamily, new nomenclature and molecular/ functional properties. *Pflugers Arch.* **2004**, *447*, 653−65.

(5) Smith, N. F.; Figg, W. D.; Sparreboom, A. Role of the liver-specific transporters OATP1B1 and OATP1B3 in governing drug elimination. *Expert Opin. Drug Metab. Toxicol.* **2005**, *1*, 429−45.

(6) Nakanishi, T.; Tamai, I. Genetic polymorphisms of OATP transporters and their impact on intestinal absorption and hepatic disposition of drugs. *Drug Metab. Pharmacokinet.* **2012**, *27*, 106−21.

(7) Niemi, M.; Pasanen, M. K.; Neuvonen, P. J. Organic anion transporting polypeptide 1B1: a genetically polymorphic transporter of major importance for hepatic drug uptake. *Pharmacol. Rev.* **2011**, *63*, 157−81.

(8) Bech-Hansen, N. T.; Till, J. E.; Ling, V. Pleiotropic phenotype of colchicine-resistant CHO cells: cross-resistance and collateral sensitivity. *J. Cell Physiol.* **1976**, *88*, 23−31.

(9) Borst, P.; Schinkel, A. H.; Smit, J. J.; Wagenaar, E.; Van Deemter, L.; Smith, A. J.; Eijdems, E. W.; Baas, F.; Zaman, G. J. Classical and novel forms of multidrug resistance and the physiological functions of P-glycoproteins in mammals. *Pharmacol. Ther.* **1993**, *60*, 289−99.

(10) Gottesman, M. M.; Pastan, I. Biochemistry of multidrug resistance mediated by the multidrug transporter. *Annu. Rev. Biochem.* **1993**, *62*, 385−427.

(11) Hofsli, E.; Nissen-Meyer, J. Reversal of drug resistance by erythromycin: erythromycin increases the accumulation of actinomycin D and doxorubicin in multidrug-resistant cells. *Int. J. Cancer* **1989**, *44*, 149−54.

(12) Kwatra, D.; Vadlapatla, R. K.; Vadlapudi, A. D.; Pal, D.; Mitra, A. K. Interaction of gatifloxacin with efflux transporters: a possible mechanism for drug resistance. *Int. J. Pharmaceutics* **2010**, *395*, 114−21.

(13) Mechetner, E. B.; Roninson, I. B. Efficient inhibition of P-glycoprotein-mediated multidrug resistance with a monoclonal antibody. *Proc. Natl. Acad. Sci. U.S.A.* **1992**, *89*, 5824−8.

(14) Roninson, I. B.; Abelson, H. T.; Housman, D. E.; Howell, N.; Varshavsky, A. Amplification of specific DNA sequences correlates with multi-drug resistance in Chinese hamster cells. *Nature* **1984**, *309*, 626−8.

(15) Ueda, K.; Okamura, N.; Hirai, M.; Tanigawara, Y.; Saeki, T.; Kioka, N.; Komano, T.; Hori, R. Human P-glycoprotein transports cortisol, aldosterone, and dexamethasone, but not progesterone. *J. Biol. Chem.* **1992**, *267*, 24248−52.

(16) Zhou, S. F. Structure, function and regulation of P-glycoprotein and its clinical relevance in drug disposition. *Xenobiotica* **2008**, *38*, 802−32.

(17) Englund, G.; Hallberg, P.; Artursson, P.; Michaelsson, K.; Melhus, H. Association between the number of coadministered P-glycoprotein inhibitors and serum digoxin levels in patients on therapeutic drug monitoring. *BMC Med.* **2004**, *2*, 8.

(18) Guengerich, F. P. Cytochrome P-450 3A4: regulation and role in drug metabolism. *Annu. Rev. Pharmacol. Toxicol.* **1999**, *39*, 1−17.

(19) Ingelman-Sundberg, M.; Sim, S. C.; Gomez, A.; Rodriguez-Antona, C. Influence of cytochrome P450 polymorphisms on drug therapies: pharmacogenetic, pharmacoepigenetic and clinical aspects. *Pharmacol. Ther.* **2007**, *116*, 496−526.

(20) Lin, J. H. Drug-drug interaction mediated by inhibition and induction of P-glycoprotein. *Adv. Drug Delivery Rev.* **2003**, *55*, 53−81.

(21) Pal, D.; Mitra, A. K. MDR- and CYP3A4-mediated drug-drug interactions. *J. Neuroimmun. Pharmacol.* **2006**, *1*, 323−39.

(22) van Waterschoot, R. A.; Lagas, J. S.; Wagenaar, E.; van der Kruijssen, C. M.; van Herwaarden, A. E.; Song, J. Y.; Rooswinkel, R. W.; van Tellingen, O.; Rosing, H.; Beijnen, J. H.; Schinkel, A. H. Absence of both cytochrome P450 3A and P-glycoprotein dramatically increases docetaxel oral bioavailability and risk of intestinal toxicity. *Cancer Res.* **2009**, *69*, 8996−9002.

(23) van Waterschoot, R. A.; Schinkel, A. H. A critical analysis of the interplay between cytochrome P450 3A and P-glycoprotein: recent insights from knockout and transgenic mice. *Pharmacol. Rev.* **2011**, *63*, 390−410.

(24) Benet, L. Z. The drug transporter-metabolism alliance: uncovering and defining the interplay. *Mol. Pharmaceutics* **2009**, *6*, 1631−43.

(25) Karlgren, M.; Vildhede, A.; Norinder, U.; Wisniewski, J. R.; Kimoto, E.; Lai, Y.; Haglund, U.; Artursson, P. Classification of inhibitors of hepatic organic anion transporting polypeptides (OATPs): influence of protein expression on drug-drug interactions. *J. Med. Chem.* **2012**, *55*, 4740−63.

(26) Li, J.; Culman, J.; Hortnagl, H.; Zhao, Y.; Gerova, N.; Timm, M.; Blume, A.; Zimmermann, M.; Seidel, K.; Dirnagl, U.; Unger, T. Angiotensin AT2 receptor protects against cerebral ischemia-induced neuronal injury. *FASEB J.* **2005**, *19*, 617−9.

(27) Ohtsuki, S.; Uchida, Y.; Kubo, Y.; Terasaki, T. Quantitative targeted absolute proteomics-based ADME research as a new path to drug discovery and development: methodology, advantages, strategy, and prospects. *J. Pharm. Sci.* **2011**, *100*, 3547−59.

(28) Shitara, Y.; Sugiyama, Y. Pharmacokinetic and pharmacodynamic alterations of 3-hydroxy-3-methylglutaryl coenzyme A (HMG-CoA) reductase inhibitors: drug-drug interactions and interindividual differences in transporter and metabolic enzyme functions. *Pharmacol. Ther.* **2006**, *112*, 71−105.

(29) Lennernas, H. Clinical pharmacokinetics of atorvastatin. *Clin. Pharmacokinet.* **2003**, *42*, 1141−60.

(30) Hochman, J. H.; Pudvah, N.; Qiu, J.; Yamazaki, M.; Tang, C.; Lin, J. H.; Prueksaritanont, T. Interactions of human P-glycoprotein with simvastatin, simvastatin acid, and atorvastatin. *Pharm. Res.* **2004**, *21*, 1686−91.

(31) Link, E.; Parish, S.; Armitage, J.; Bowman, L.; Heath, S.; Matsuda, F.; Gut, I.; Lathrop, M.; Collins, R. SLCO1B1 variants and statin-induced myopathy–a genomewide study. *N. Engl. J. Med.* **2008**, *359*, 789−99.

(32) Neuvonen, P. J.; Niemi, M.; Backman, J. T. Drug interactions with lipid-lowering drugs: mechanisms and clinical relevance. *Clin. Pharmacol. Ther.* **2006**, *80*, 565−81.
(33) Niemi, M. Transporter pharmacogenetics and statin toxicity. *Clin. Pharmacol. Ther.* **2010**, *87*, 130−3.
(34) Crespi, C. L.; Fox, L.; Stocker, P.; Hu, M.; Steimel, D. T. Analysis of drug transport and metabolism in cell monolayer systems that have been modified by cytochrome P4503A4 cDNA-expression. *Eur. J. Pharm. Sci.* **2000**, *12*, 63−8.
(35) Fahrmayr, C.; Konig, J.; Auge, D.; Mieth, M.; Fromm, M. F. Identification of drugs and drug metabolites as substrates of multidrug resistance protein 2 (MRP2) using triple-transfected MDCK-OATP1B1-UGT1A1-MRP2 cells. *Br. J. Pharmacol.* **2012**, *165*, 1836−47.
(36) Tang, F.; Horie, K.; Borchardt, R. T. Are MDCK cells transfected with the human MDR1 gene a good model of the human intestinal mucosa? *Pharm. Res.* **2002**, *19*, 765−72.
(37) Kwatra, D.; Budda, B.; Vadlapudi, A. D.; Vadlapatla, R. K.; Pal, D.; Mitra, A. K. Transfected MDCK Cell Line with Enhanced Expression of CYP3A4 and P-Glycoprotein as a Model To Study Their Role in Drug Transport and Metabolism. *Mol. Pharmaceutics* **2012**, *9*, 1877−1866.
(38) Ahlin, G.; Hilgendorf, C.; Karlsson, J.; Szigyarto, C. A.; Uhlen, M.; Artursson, P. Endogenous gene and protein expression of drug-transporting proteins in cell lines routinely used in drug discovery programs. *Drug Metab. Dispos.* **2009**, *37*, 2275−83.
(39) Karlgren, M.; Ahlin, G.; Bergstrom, C. A.; Svensson, R.; Palm, J.; Artursson, P. In vitro and in silico strategies to identify OATP1B1 inhibitors and predict clinical drug-drug interactions. *Pharm. Res.* **2012**, *29*, 411−26.
(40) Konig, J.; Cui, Y.; Nies, A. T.; Keppler, D. A novel human organic anion transporting polypeptide localized to the basolateral hepatocyte membrane. *Am J Physiol Gastrointest Liver Physiol* **2000**, *278*, G156−64.
(41) Wang, Y.; Liao, M.; Hoe, N.; Acharya, P.; Deng, C.; Krutchinsky, A. N.; Correia, M. A. A role for protein phosphorylation in cytochrome P450 3A4 ubiquitin-dependent proteasomal degradation. *J. Biol. Chem.* **2009**, *284*, 5671−84.
(42) Gillen, C. M.; Forbush, B., 3rd Functional interaction of the K-Cl cotransporter (KCC1) with the Na-K-Cl cotransporter in HEK-293 cells. *Am. J. Physiol.* **1999**, *276* (2 Pt 1), C328−36.
(43) Watanabe, T.; Kusuhara, H.; Maeda, K.; Kanamaru, H.; Saito, Y.; Hu, Z.; Sugiyama, Y. Investigation of the rate-determining process in the hepatic elimination of HMG-CoA reductase inhibitors in rats and humans. *Drug Metab. Dispos.* **2010**, *38*, 215−22.
(44) Lins, R. L.; Matthys, K. E.; Verpooten, G. A.; Peeters, P. C.; Dratwa, M.; Stolear, J. C.; Lameire, N. H. Pharmacokinetics of atorvastatin and its metabolites after single and multiple dosing in hypercholesterolaemic haemodialysis patients. *Nephrol. Dial. Transplant* **2003**, *18*, 967−76.
(45) Schachter, M. Chemical, pharmacokinetic and pharmacodynamic properties of statins: an update. *Fundam. Clin. Pharmacol.* **2005**, *19*, 117−25.
(46) Chen, C.; Mireles, R. J.; Campbell, S. D.; Lin, J.; Mills, J. B.; Xu, J. J.; Smolarek, T. A. Differential interaction of 3-hydroxy-3-methylglutaryl-coa reductase inhibitors with ABCB1, ABCC2, and OATP1B1. *Drug Metab. Dispos.* **2005**, *33*, 537−46.
(47) Jacobsen, W.; Kuhn, B.; Soldner, A.; Kirchner, G.; Sewing, K. F.; Kollman, P. A.; Benet, L. Z.; Christians, U. Lactonization is the critical first step in the disposition of the 3-hydroxy-3-methylglutaryl-CoA reductase inhibitor atorvastatin. *Drug Metab. Dispos.* **2000**, *28*, 1369−78.
(48) Amundsen, R.; Christensen, H.; Zabihyan, B.; Asberg, A. Cyclosporine A, but not tacrolimus, shows relevant inhibition of organic anion-transporting protein 1B1-mediated transport of atorvastatin. *Drug Metab. Dispos.* **2010**, *38*, 1499−504.
(49) Wu, X.; Whitfield, L. R.; Stewart, B. H. Atorvastatin transport in the Caco-2 cell model: contributions of P-glycoprotein and the proton-monocarboxylic acid co-transporter. *Pharm. Res.* **2000**, *17*, 209−15.
(50) Fahrmayr, C.; Konig, J.; Auge, D.; Mieth, M.; Munch, K.; Segrestaa, J.; Pfeifer, T.; Treiber, A.; Fromm, M. Phase I and II metabolism and MRP2-mediated export of bosentan in a MDCKII-OATP1B1-CYP3A4-UGT1A1-MRP2 quadruple-transfected cell line. *Br. J. Pharmacol.* **2013**, *169*, 21−33.
(51) Di, L.; Whitney-Pickett, C.; Umland, J. P.; Zhang, H.; Zhang, X.; Gebhard, D. F.; Lai, Y.; Federico, J. J., 3rd; Davidson, R. E.; Smith, R.; Reyner, E. L.; Lee, C.; Feng, B.; Rotter, C.; Varma, M. V.; Kempshall, S.; Fenner, K.; El-Kattan, A. F.; Liston, T. E.; Troutman, M. D. Development of a new permeability assay using low-efflux MDCKII cells. *J. Pharm. Sci.* **2011**, *100*, 4974−85.
(52) Liao, M.; Raczynski, A. R.; Chen, M.; Chuang, B. C.; Zhu, Q.; Shipman, R.; Morrison, J.; Lee, D.; Lee, F. W.; Balani, S. K.; Xia, C. Q. Inhibition of hepatic organic anion-transporting polypeptide by RNA interference in sandwich-cultured human hepatocytes: an in vitro model to assess transporter-mediated drug-drug interactions. *Drug Metab. Dispos.* **2010**, *38*, 1612−22.
(53) Williamson, B.; Soars, A. C.; Owen, A.; White, P.; Riley, R. J.; Soars, M. G. Dissecting the relative contribution of OATP1B1-mediated uptake of xenobiotics into human hepatocytes using siRNA. *Xenobiotica* **2013**, DOI: 10.3109/00498254.2013.776194.
(54) Yue, W.; Abe, K.; Brouwer, K. L. Knocking down breast cancer resistance protein (Bcrp) by adenoviral vector-mediated RNA interference (RNAi) in sandwich-cultured rat hepatocytes: a novel tool to assess the contribution of Bcrp to drug biliary excretion. *Mol. Pharmaceutics* **2009**, *6*, 134−43.
(55) Noe, J.; Portmann, R.; Brun, M. E.; Funk, C. Substrate-dependent drug-drug interactions between gemfibrozil, fluvastatin and other organic anion-transporting peptide (OATP) substrates on OATP1B1, OATP2B1, and OATP1B3. *Drug Metab. Dispos.* **2007**, *35*, 1308−14.
(56) Kameyama, Y.; Yamashita, K.; Kobayashi, K.; Hosokawa, M.; Chiba, K. Functional characterization of SLCO1B1 (OATP-C) variants, SLCO1B1*5, SLCO1B1*15 and SLCO1B1*15+C1007G, by using transient expression systems of HeLa and HEK293 cells. *Pharmacogenet. Genomics* **2005**, *15*, 513−22.
(57) Pasanen, M. K.; Neuvonen, M.; Neuvonen, P. J.; Niemi, M. SLCO1B1 polymorphism markedly affects the pharmacokinetics of simvastatin acid. *Pharmacogenet. Genomics* **2006**, *16*, 873−9.